



The effect of bacterial cellulose membrane compared with collagen membrane on guided bone regeneration

So-Hyoun Lee^{1†}, Youn-Mook Lim^{2†}, Sung In Jeong^{2†}, Sung-Jun An², Seong-Soo Kang³,
Chang-Mo Jeong¹, Jung-Bo Huh^{1*}

¹Department of Prosthodontics, Dental Research Institute, Biomedical Research Institute, School of Dentistry, Pusan National University, YangSan, Republic of Korea

²Advanced Radiation Technology Institute, Korea Atomic Energy Research Institute, Jeongeup, Republic of Korea

³Department of Veterinary Surgery, College of Veterinary Medicine, Chonnam National University, Gwangju, Republic of Korea

PURPOSE. This study was to evaluate the effects of bacterial cellulose (BC) membranes as a barrier membrane on guided bone regeneration (GBR) in comparison with those of the resorbable collagen membranes. **MATERIALS AND METHODS.** BC membranes were fabricated using biomimetic technology. Surface properties were analyzed, Mechanical properties were measured, *in vitro* cell proliferation test were performed with NIH3T3 cells and *in vivo* study were performed with rat calvarial defect and histomorphometric analysis was done. The Mann-Whitney U test and the Wilcoxon signed rank test was used ($\alpha < .05$). **RESULTS.** BC membrane showed significantly higher mechanical properties such as wet tensile strength than collagen membrane and represented a three-dimensional multilayered structure cross-linked by nano-fibers with 60 % porosity. *In vitro* study, cell adhesion and proliferation were observed on BC membrane. However, morphology of the cells was found to be less differentiated, and the cell proliferation rate was lower than those of the cells on collagen membrane. *In vivo* study, the grafted BC membrane did not induce inflammatory response, and maintained adequate space for bone regeneration. An amount of new bone formation in defect region loaded with BC membrane was significantly similar to that of collagen membrane application. **CONCLUSION.** BC membrane has potential to be used as a barrier membrane, and efficacy of the membrane on GBR is comparable to that of collagen membrane. [J Adv Prosthodont 2015;7:484-95]

KEY WORDS: Bacterial cellulose membrane; Collagen membrane; Guided bone regeneration; Rat calvarial defect

Corresponding author:

Jung-Bo Huh
Department of Prosthodontics, Dental Research Institute, Biomedical Research Institute, School of Dentistry, Pusan National University, 20, Geumo-ro, Mulgeum-eup, Yangsan 50612, Rep. of Korea
Tel. 82 55 360 5146; e-mail, huhjb@pusan.ac.kr
Received October 1, 2015 / Last Revision November 30, 2015 / Accepted December 1, 2015

© 2015 The Korean Academy of Prosthodontics
This is an Open Access article distributed under the terms of the Creative Commons Attribution Non-Commercial License (<http://creativecommons.org/licenses/by-nc/3.0>) which permits unrestricted non-commercial use, distribution, and reproduction in any medium, provided the original work is properly cited.

† These authors contributed equally to this work.
This study was supported by iPET (Korea Institute of Planning and Evaluation for Technology in Food, Agriculture, Forestry and Fisheries), Ministry of Agriculture, Food and Rural Affairs (No. 2013100659), and supported by a grant from the Korean Health Technology R&D Project through the Korean Health Industry Development Institute (KHIDI), funded by the Korean Ministry of Health & Welfare (grant number: HI14C3309).

INTRODUCTION

In dental implant and prosthetic dentistry, maintaining residual alveolar bone volume after tooth-loss is crucial in order to increase clinical success; however, it often faces limitations due to some factors such as infection, external injury, and other lesions.¹ As importance of alveolar bone regeneration in bone defect became more emphasized, various bone regeneration techniques including block bone graft, ridge splitting, distraction osteogenesis, and guided bone regeneration (GBR) have been introduced.²⁻⁴ Among these treatment techniques, GBR which was developed by the study of Ashely *et al.*⁵ using cellulose acetate filter to induce regeneration of tendon is the most commonly used these days. Many studies have confirmed the predicted efficacy of GBR^{6,7}: GBR utilizes a barrier membrane, restrict-

ing a down-growth of connective and epithelial tissues inside of bone defect, maintaining a space for new bone formation, and ultimately promoting bone regeneration.⁴ Scantlebury *et al.*⁸ suggested five prerequisites for a barrier membrane: biocompatibility, cell-occlusiveness, space-making, tissue integration, and clinical manageability. Buser *et al.*⁹ underlined that successful bone regeneration by GBR can be achieved when a barrier membrane has sufficient mechanical strength, porosity, and blood clot stabilizing enhancers.

Barrier membranes can be categorized into resorbable and non-resorbable barrier membranes.¹⁰⁻¹² Expanded polytetrafluoroethylene (e-PTFE) and titanium mesh are the standard non-resorbable barrier membranes. Although these membranes show excellent mechanical strength and space-making ability, they also have limitations: a second operation is required for membrane removal, and premature membrane exposure can cause some complications such as infection and bone loss.¹³⁻¹⁵ Resorbable barrier membrane such as degradable materials like collagen,^{16,17} polyactin acid, polyglycolic acid,^{18,19} and inorganic ceramics²⁰ have been introduced in order to overcome these limitations of non-resorbable barrier membranes. Collagen is a major component in natural extracellular matrix (ECM); tissue-derived collagen-based membranes have been chosen as important alternatives to synthetic polymers for their excellent cell affinity and biocompatibility.²¹ In addition, the collagen-based barrier membranes allow some degree of manageability and outstanding tissue-integration.²² On the other hand, it is difficult to predict the degradation period and absorption rate in clinical settings and to examine the regenerated bone tissue. When exposed to moisture or blood, the membranes also show a decreased space-making ability due to their poor mechanical strength.^{11,23} Furthermore, high cost and poor definition of their commercial sources are the limitations of collagen-based barrier membranes.²⁴

As barrier membranes become universally applicable, excellent biological activity and low cost are acknowledged as additional prerequisites along the other prerequisites mentioned earlier.²⁵ Accordingly, some studies in tissue engineering field have begun to focus on application of bacterial cellulose (BC) as a barrier membrane material. BC produced by Bacterium *Gluconacetobacter hansenii* TL-2 is a natural polysaccharide with β -(1,4) glycosidic bonds. It performs as a natural extracellular matrix (ECM) mimic, exhibiting advantageous properties including ultrafine, highly-hydrated microfibril network structure made up of 99% water and high-burst pressure.^{26,27} Unlike vegetable cellulose, BC is a pure form of cellulose without any impurities, for example, hemicellulose, pectin, lignin, and biogenic product; thus, its high purity can be achieved through a refining process.^{28,29} Moreover, BC is widely utilized in bone, vascular, cartilage, skin, and various tissue engineering scaffolds since it shows outstanding biocompatibility without eliciting cytotoxicity or immune response.³⁰⁻³³ Bacterial cellulose is morphologically similar to collagen

that possesses a nano-sized structure.³⁴ Therefore, many studies attempted to use BC as a barrier membrane material in GBR, examining its mechanical properties, nanostructure analysis, *in vitro* cell adhesion and proliferation, and *in vivo* bone regeneration.^{26,31,32,35} However, even though comparing the clinical effects of BC membrane to those of other conventional barrier membranes used in GBR is essential to provide evidences for clinical efficacy of BC membrane, few studies were hardly made.

Therefore, in this present study, bone materials and two different membranes including BC and collagen membranes were applied in rat calvarial defect model. After four and eight weeks of recovery period, the effectiveness of BC membrane on bone formation was compared to that of collagen membrane through histometric analysis.

MATERIALS AND METHODS

Collagen membrane (GENOSS, Suwon, Korea) and bacterial cellulose membrane (Jadam Co. Jeju, South Korea) were chosen as barrier membranes in this experiment. Bacterial cellulose membrane manufactured with a metabolic product of *Gluconacetobacter hansenii* TL-2C and fermented Jeju citrus peel. The bacterial strain, *Gluconacetobacter hansenii* TL-2C was incubated for 7 days in a static culture containing 0.3% (w/w) fermented citrus solution and 5% (w/w) sucrose. The pH was adjusted to 4.5 with acetic acid. The obtained gel-like pellicles of BC were purified by immersion in deionized water at 90°C for 2 hours and then boiled in a 0.5 M aqueous solution of NaOH for 15 minutes to remove bacterial cell remains. The BC was then washed with deionized water several times and soaked in 1% NaOH for 2 days. Finally, the BC pellicles were washed free of alkali. All other reagents and solvents were of analytical grade and used without further purification.

SEM images of the BC and collagen membrane were obtained with SEM equipment (JSM-6390, JEOL, Tokyo, Japan) operating at 10 kV and 10 - 12 mm in distance. Samples were deposited on a steel plate and coated with gold for 60 seconds.

The BC and collagen membranes were evaluated for their mechanical properties by using Universal Testing Instrument (Instron 5569, Instron Corp., Canton, OH, USA) with 5 kN load cell and crosshead speed of 10 mm/min. The samples were cut into 5 mm width \times 30 mm length. This method specifies a procedure for determination of the wet tensile strength by measuring the tensile strength of the samples after 10 minutes soaking in water.

The porosity and pore-size distribution of BC and collagen membrane were characterized by mercury intrusion porosimetry measured with AutoPore IV 9500 mercury porosimeter of Micromeritics Instrument Corporation., USA. The maximum application pressure of mercury was 31,000 psi (214 MPa). The mercury-intrusion measurements were corrected for the compression of liquid mercury and the expansion of the penetrometer (sample holder). Detailed working mechanism of the mercury porosimeter

can be obtained from Micromeritics Instrument Corp.

NIH3T3 cells (ATCC® CRL-1658™, mouse embryo fibroblast) were cultured in Dulbecco's Modified Eagle Medium with 4.5 g·L⁻¹ glucose (DMEM-HG, Gibco BRL, Grand Island, NY, USA) supplemented with 10% fetal bovine serum and 1% penicillin/streptomycin in a CO₂ incubator at 37°C with 5% CO₂, 95% humidity, and the medium was changed every two days. The NIH3T3 cells were used at passages 5 and 6 for all experiments.

Cell proliferation was measured using a Cell Counting Kit-8 assay (CCK-8, Dojindo Laboratories, Kumamoto, Japan). NIH3T3 cells were seeded at a density of 1×10^5 cells·well⁻¹ on a bacterial cellulose and collagen membrane surfaces and then cultured for 1, 3, and 7 day. After incubation period, the culturing media were exchanged with culture medium containing 10% cck-8 solution. Then, while maintaining under the same condition for 1.5 hours, the absorbance of the cck-8 solution was measured at 450 nm with a UV-Vis spectrophotometer (MQX 200 model, Bio-Tek Instruments, Winooski, VT, USA). All experiments were performed in triplicate.

The cell nucleus and F-actin were stained to evaluate the morphology of cells on the BC and collagen membranes. After cell-culturing for 24 hours, the samples were fixed using 3.7% MeOH-free formaldehyde in PBS for 10 min at 37°C, and then following a wash in PBS, the samples were permeabilized in cytoskeleton (CSK) buffer (10.3 g sucrose, 0.292 g NaCl, 0.06 g MgCl₂, 0.476 g HEPES buffer, 0.5 ml Triton X-100, in 100 mL water, pH7.2) for 10 minutes at 4°C. The cells were blocked in blocking buffer (1% BSA in PBS) for 1 hour at 37°C. Then, the samples were incubated with Rhodamine-phalloidin (1:100) (Molecular probe, Eugene, OR, USA) and Hoechst 33258 (1:1000) (Molecular probes, Eugene, OR, USA), a nuclear stain, for 1 hour at 37°C. Following a wash in PBS, the samples were mounted on glass slides. Fluorescent images of stained cells on BC sheets were acquired using a Laser Scanning Confocal Microscope (LSM 510, Zeiss, Jena, Germany). The projected cell area from the acquired images was analyzed using Image proPlus 4.5 (Media cybernetics, Silver Springs, MD, USA).

Samples of BC and collagen membrane were punched and sterilized as 70% EtOH. NIH3T3 cells were seeded at a concentration of 1×10^5 cells·well⁻¹ on the sample surface. After 24 hours of cell culture, the samples were washed three times with PBS. The cells were fixed by adding 4% paraformaldehyde in PBS for 30 min at room temperature. They were rinsed with PBS for 5 minutes, and then the samples were dehydrated by using an ethanol gradient (50, 70, 80, 95, and 100% EtOH for 10 minutes per step). The samples were dried with the Hexamethyldisilazane (HMDS) chemical drying series (3:1, 1:1, 1:3 EtOH:HMDS for 15 minutes, and 100% HMDS allow to air dry). Afterwards, the samples were analyzed with FE-SEM (Field Emission Scanning Electron Microscope, Hitachi S-4800, Hitachi, Tokyo, Japan).

Twenty four male Sprague-Dawley rats (250-300 g in

weight) were chosen. Animals were caged individually under standard laboratory conditions in plastic cages. They had free water access and standard laboratory pellets. Animal selection, management, care, preparation for surgery, and the surgical protocol were carried out, following the guidelines from Animal Experimentation of the Korean Atomic Energy Research Institute (KAERI-IACUC-2013-004).

After intramuscularly injecting a mixture of xylazine (Rumpun, Bayer Korea, Seoul) and Tiletamin-zolazepam (Zoletil, Vibac Laboratories, Carros, France), the operation was executed under general anesthesia. The shaved surgical site at cranium was disinfected with Betadine, and 2% lidocaine HCL (Yu-Han Co., Gunpo, South Korea) was administered for local anesthesia. After incising into U-shape, a full-thickness flap of skin and periosteum was reflected. In the middle of cranium, 8 mm circular and transosseous, standardized defect was created with a trephine bur (3i Implant Innovation, Palm Beach Garden, FL, USA). During drilling, the surgical site was washed with saline. After dismissing the trephined bony disk, experimental and control materials were brought into the prepared sites. 12 animals were distributed to each study group. After treating 0.12 mg hydroxyapatite (HA)/TCP bone graft material (Bio-C, Cowellmedi Implant, Seoul), the defect site of each animal was enclosed with 10 × 10 mm of collagen membrane or BC membrane. The 4-0 absorbable suture (Vicryl®, Ethicon, Somerville, NJ, USA) was used to suture the surgical sites (Fig. 1). 6 animals of each group had a healing period for 4 weeks, and the remaining 6 animals had a healing period for 8 weeks.

With rapid acid decalcification reagents and 14% ethylenediaminetetraacetic acid (EDTA), the calvarial tissue specimens of rats were decalcified. Paraffin was used to embed the specimens, and the center of calvarial defect was sectioned at 5 μm. The most centered sections from each block were stained with hematoxylin-eosin. With a light microscope (BX50, Olympus, Tokyo, Japan), the stained slides were observed, and their images were saved digitally. An image analysis program (Image-Pro Plus, Media Cybernetic, Silver Spring, MD, USA) was used to obtain computer-assisted histometric measurements in order to capture images of new bone and residual biomaterial areas. With the following of the previous study²⁴ new bone and residual biomaterial percentages in defect area were obtained.

All of the quantitative results were obtained from triplicate samples. Data are expressed as mean ± SD. Since not all the group followed a regular distribution, non-parametric tests were performed. Statistical analysis was performed using SPSS ver. 21.0 (SPSS, Chicago, IL, USA). The Mann-Whitney U test was used to determine differences between measurements taken within the groups, and the Wilcoxon signed rank test was used to determine differences between measurements taken at 4 and 8 weeks after surgery within each groups. Statistical significance was accepted for *P* values < .05.

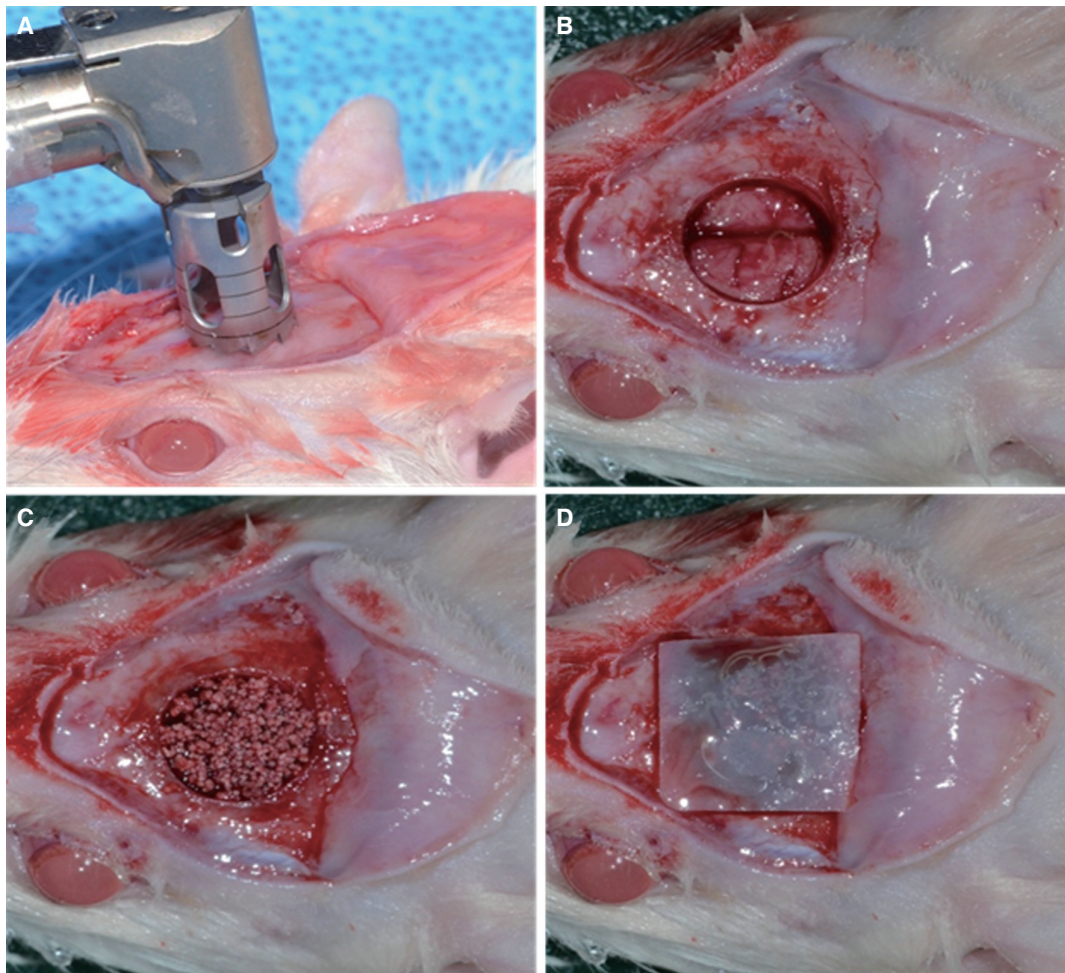


Fig. 1. *In vivo* operation procedure full-thickness rat calvarial defects. (A, B) In the middle of cranium, 8 mm-diameter defect was created with a trephine bur. (C) The defect site treated with bone graft material and (D) enclosed with barrier membrane (Collagen membrane (GENOSS, Suwon, Korea) or bacterial cellulose membrane (Jadam Co. Jeju, South Korea)).

RESULTS

The SEM images of the two different membranes are displayed in Fig. 2. In the morphologic analysis, distinct differences were not found between the collagen membrane (A, C) and BC membrane (B, D). In case of surface images (A) and (B), both samples confirmed a porous structure made up of the entangled nano-sized fibers. In case of cross-section images (C) and (D), both samples had a multilayered lamellar structure. Especially, image (D) showed a three-dimensional structure of BC cross-linked by nano-fibers.

The mechanical properties of the membranes including their tensile strength, modulus, and strain at failure, are shown in Fig. 3. The tensile stress of BC and collagen membranes was 2.88 ± 0.33 MPa and 2.34 ± 0.09 MPa respectively. The tensile strain was measured to be $3.25 \pm 0.39\%$ and $1.85 \pm 0.10\%$ respectively, and Young's modulus was 644.71 ± 15.23 MPa and 520.21 ± 8.77 MPa respective-

ly. BC showed significantly higher values of tensile strength, strain, and modulus than collagen membranes. We could confirm that the BC has a better mechanical property than the collagen membranes ($P < .05$).

Fig. 3. Mechanical properties (A) tensile stress, (B) tensile strain and (C) young's modulus diagram of collagen membranes and BC membrane after 10 minutes soaking in water.

The porous structure of BC and collagen membranes was each of 59.35% and 34.35%, the diameter of the pore was each of $26 \mu\text{m}$ and $19 \mu\text{m}$, and the total pore area was each of 0.048 m^2 and 0.014 m^2 .

The CCK-8 assay of cells on the BC and collagen membrane substrates was carried out to test the cell proliferation and adhesion. As shown in Fig. 4, the proliferation of NIH3T3 cells on both BC and collagen membrane increased throughout the incubation period for up to 7 days. After one day, the proliferation of NIH3T3 cells on BC, $41.12 \pm$

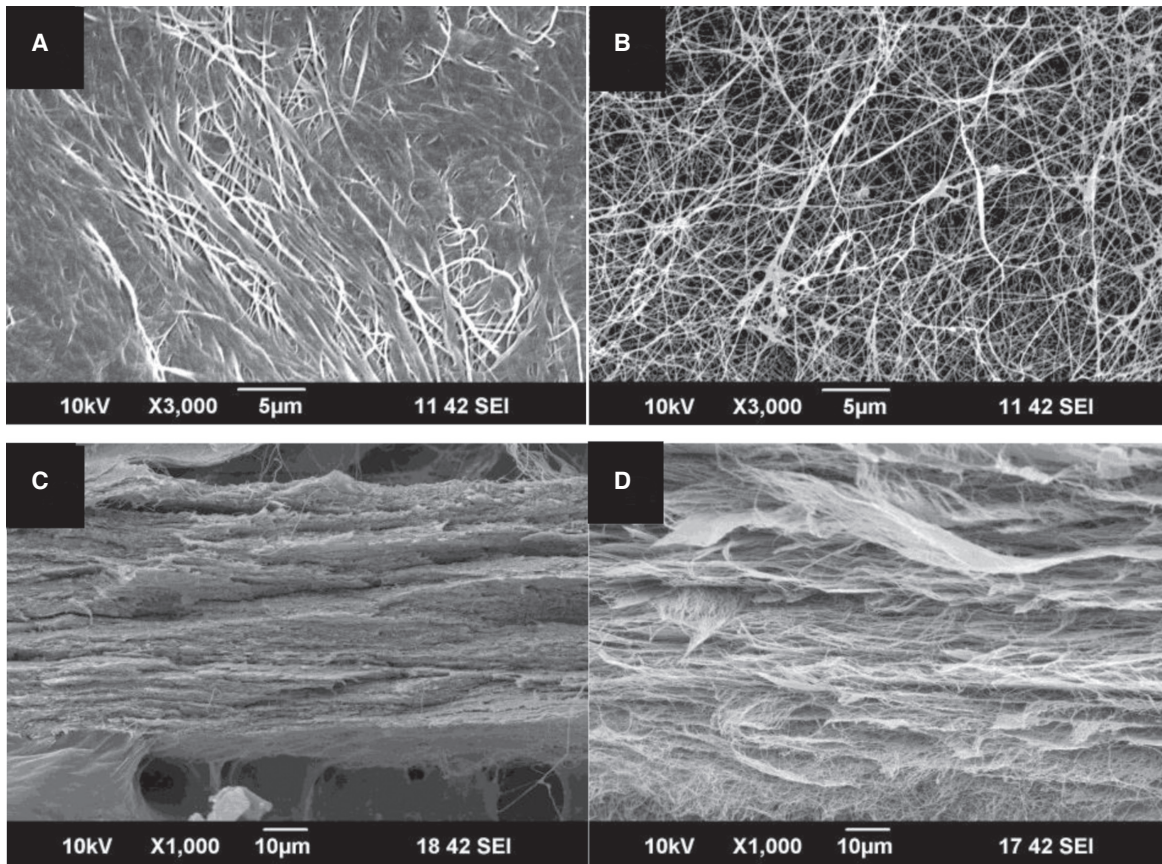


Fig. 2. SEM micrographs of (A, C) collagen membrane and (B, D) bacterial cellulose membrane. The (A, B) surface side and (C, D) cross-section side showed nano porous structure (original magnification: $\times 3,000$ [(A), (B)], $\times 1,000$ [(C), (D)]).

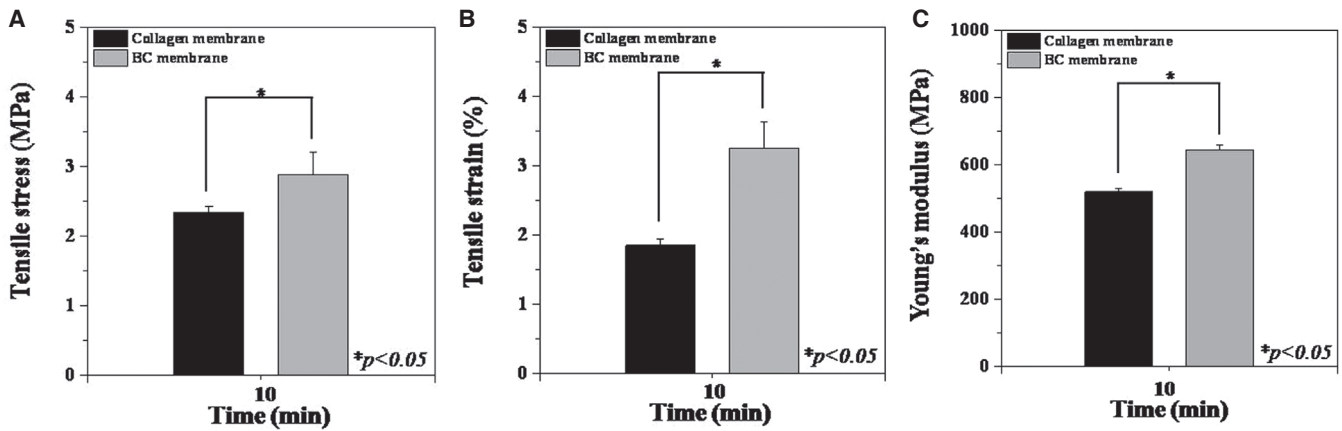


Fig. 3. Mechanical properties (A) tensile stress, (B) tensile strain and (C) Young's modulus diagram of collagen membranes and BC membrane after 10 minutes soaking in water.

0.33%, did not show significant difference compared to collagen membrane, $47.16 \pm 0.61\%$. However, after 3 days, BC, $50.22 \pm 0.52\%$, displayed significantly lower cell proliferation than Collagen membrane, $89.84 \pm 0.12\%$ ($P < .05$). After a maximum incubation period of 7 days, cell proliferation on BC, $62.87 \pm 0.24\%$, remained significantly lower than that on collagen membrane, $113.95 \pm 0.26\%$ ($P < .05$).

The morphology of adherent cells on the membranes after 7 day is shown in Fig. 5 and Fig. 6. The ability of membranes to support NIH3T3 cells adhesion was evaluated by F-actin staining and SEM. The cells on BC membrane maintained a round shape, and actin stress fibers were mainly localized in the periphery of the cell (Fig. 5C, Fig. 5D, Fig. 6B). However, the cells on the collagen membrane were more spread out than those on the BC membrane, and typical long and straight actin stress fibers of the cells were observed on membrane (Fig. 5A, Fig. 5B, Fig. 6A).

Healing was uneventful in all animals. After a healing

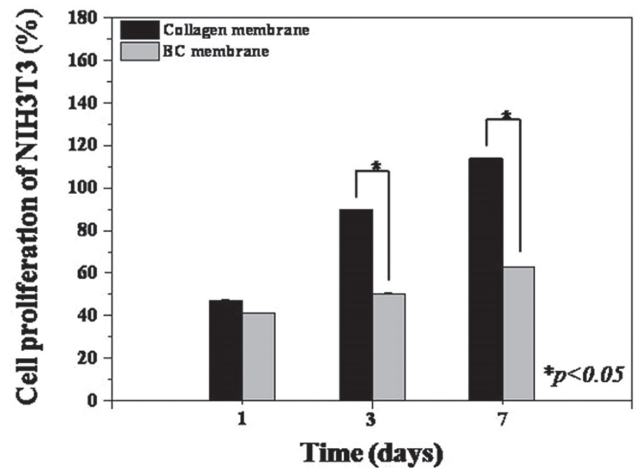


Fig. 4. Proliferation of NIH3T3 cells cultured on BC and collagen membrane prepared at various fluorescence as quantified by a CCK-8 assay at 1, 3 and 7 days.

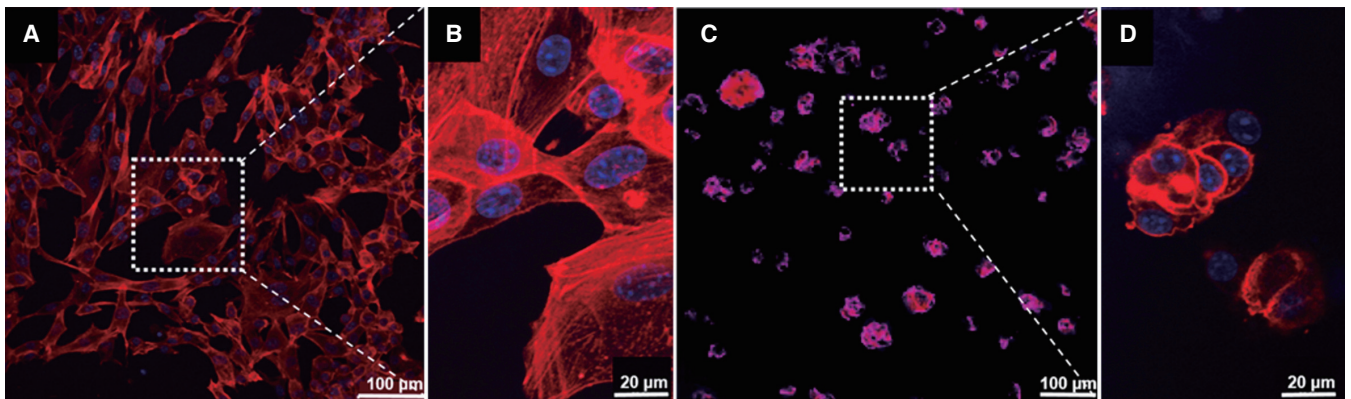


Fig. 5. Immunofluorescent staining image of the adherent cells on (A, B) collagen membrane, and (C, D) BC membrane after 7 days measured by a confocal microscope (original magnification: $\times 200$ [(A), (C)], $\times 400$ [(B)]).

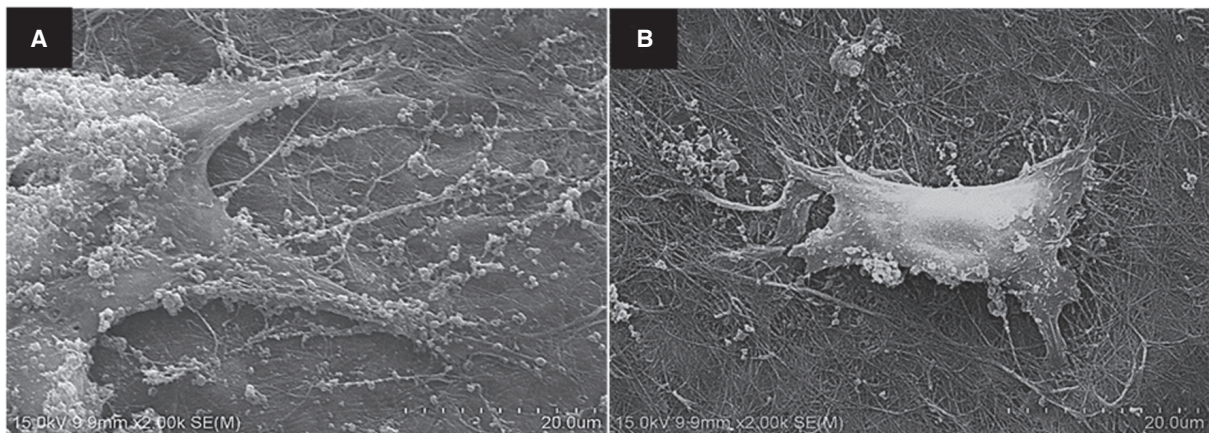


Fig. 6. SEM image of the adherent cells on (A) collagen membrane (B) BC membrane after 7 days (original magnification: $\times 2,000$ [(A), (B)]).

period of 4 weeks, the defect region was limited by a membrane in the BC and collagen membrane groups, and the space formed under the membrane was charged with fibrous connective tissue and bone-like materials. Blood vessels were invading the defect area, especially inside of the membrane (Fig. 7). In addition, both the BC and collagen membrane groups showed new bone formation derived from existing old bone and around the bone grafted materials, but most of this new bone tissue was immature. In the defect area, mesenchymal cells randomly located within col-

lagen fibers of fibrous connective tissue and osteoblasts derived from the mesenchymal cells nearby were observed around the newly formed bone matrix (osteoid). The lightly stained matrix is osteoid. (Fig. 7E, Fig. 7F). At 8 weeks in this group, both the BC and collagen membranes remained and revealed good tissue integration (Fig. 8A, Fig. 8B). New bone tissue of the BC and collagen membrane groups was more mature, and there was more new bone formation within the defect margins (Fig. 8C, Fig. 8D). Osteoblast rimming was observed around the newly formed bone

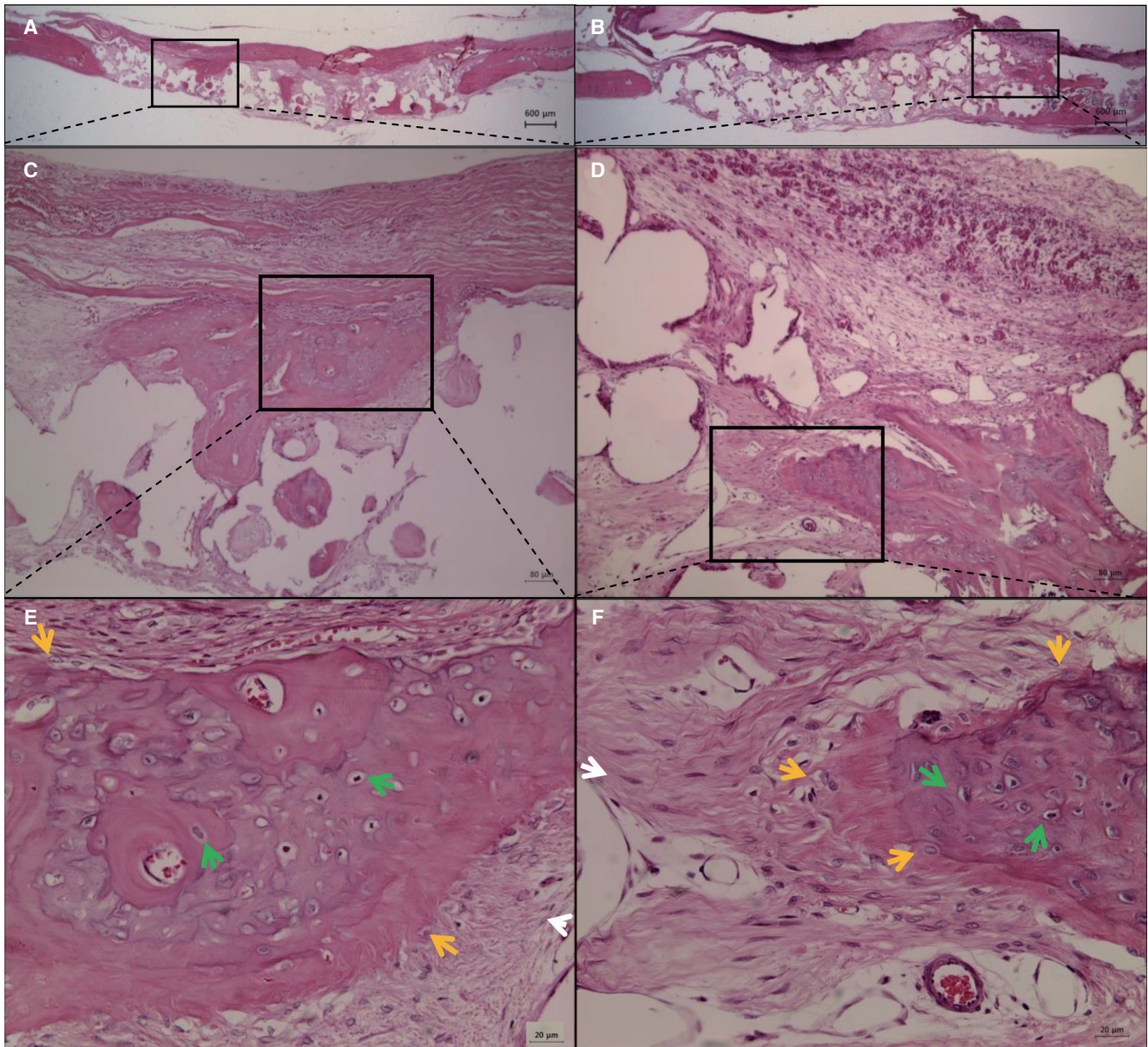


Fig. 7. H&E staining of histological sections of defect sites at 4 weeks after surgery. New bone formation and fibrous connective tissue were observed in the collagen group (A, C, E) and in the BC group (B, D, F). The membrane was not absorbed. The rectangles in (A, B, C, D) indicate the new bone formation. white arrow: mesenchymal cell; black asterisk: blood vessel; yellow asterisk: osteoid; yellow arrow: osteoblast; green arrow: osteocyte within a lacuna; (original magnification: $\times 12.5$ [(A), (B)], $\times 100$ [(C), (D)], $\times 400$ [(E), (F)]).

matrix. In particular, active cuboidal osteoblasts and osteocytes were found around the bone-like materials and new bone. Osteocytes within lacunae were found in the more heavily stained bone matrix (Fig. 8E, Fig. 8F). After 8 weeks of healing, in the BC and collagen membrane groups, a greater amount of fibrous connective tissue and new bone formation was observed than at 4 weeks. However, the histometric measurements of each group showed no significant difference in new bone formation (%) between week 4 and week 8, and a significant difference was not observed

between BC and collagen membranes either. The histometric measurements are summarized in Table 1. In comparison of groups with different membrane materials, mean neo-tissue (NT)/ new-bone (NB) area (%) was no significantly between collagen and BC groups at 4 weeks (collagen : $17.13 \pm 9.65\%$, BC : $15.82 \pm 2.95\%$) and 8 weeks (collagen : $17.47 \pm 5.09\%$, BC : $16.78 \pm 5.27\%$) ($P > .05$). As comparing a healing period within a group, new-bone area (%) of collagen and BC groups was maintained throughout the healing period for up to 8 weeks.

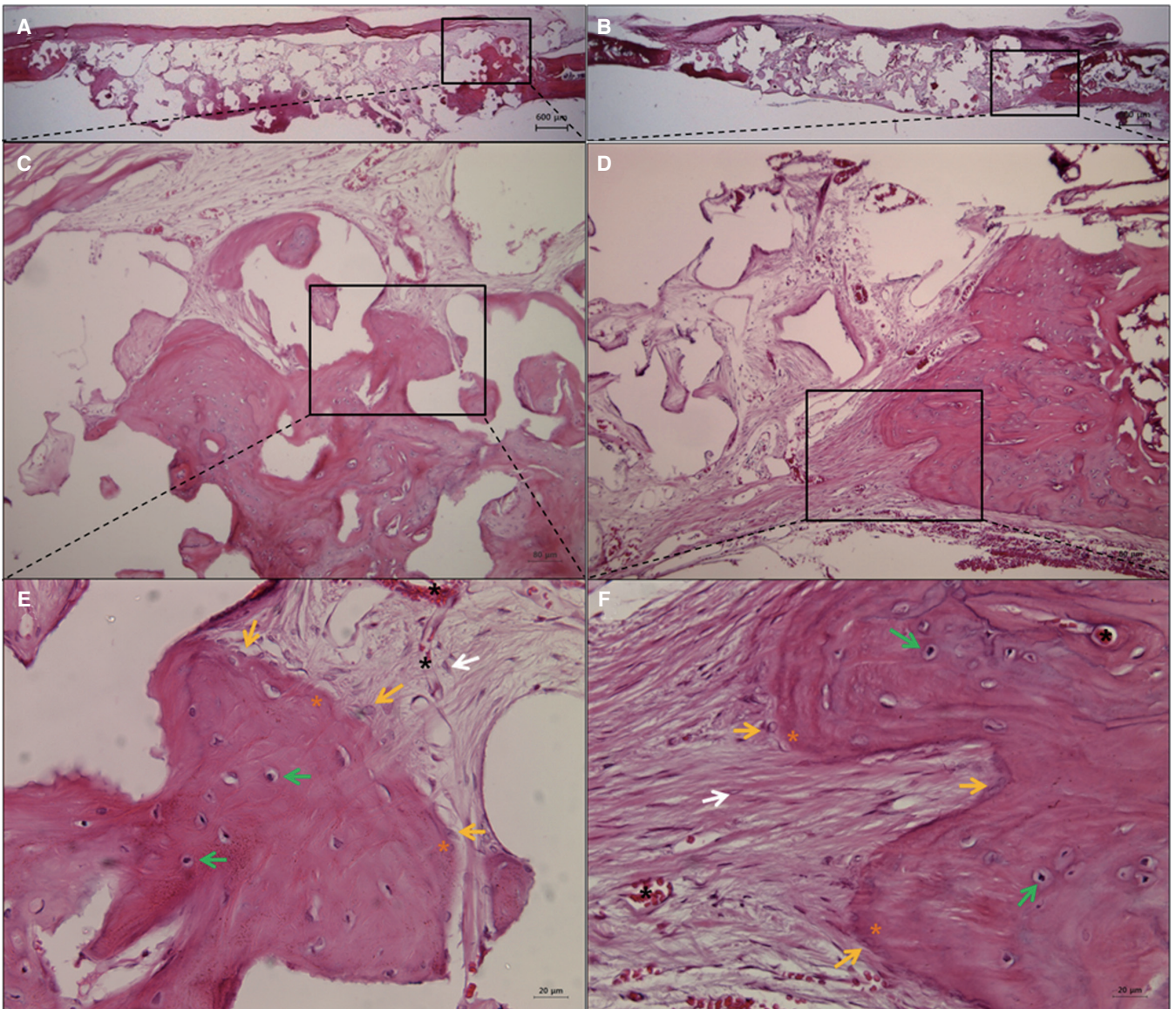


Fig. 8. H&E staining of histological sections of defect sites at 8 weeks after surgery. New bone formation and fibrous connective tissue were observed in the collagen group (A, C, E) and in the BC group (B, D, F). The membrane was not absorbed. The rectangles in (A, B, C, D) indicate the new bone formation. white arrow: mesenchymal cell; black asterisk: blood vessel; yellow asterisk: osteoid; yellow arrow: osteoblast; green arrow: osteocyte within a lacuna. (original magnification: $\times 12.5$ [(A), (B)], $\times 100$ [(C), (D)], $\times 400$ [(E), (F)]).

Table 1. Mean (\pm SD) of neo-tissue (NT)/ new-bone (NB) area (%) to groups at 4 and 8 weeks after surgery

Group (membrane)	4 weeks	8 weeks	P†
Collagen	17.13 \pm 9.65	17.47 \pm 5.09	.917
BC	15.82 \pm 2.95	16.78 \pm 5.27	.753
P*	.937	.818	

The symbols '*' and '†' indicate statistical significance; the collagen vs BC groups, respectively ($P < .05$).

DISCUSSION

In this study, application of bacterial cellulose (BC) membrane on rat calvarial bone defect area manifested a high degree of biocompatibility and tissue integration, similarly to collagen membrane. This corresponds to the result from the previous study by Helenius *et al.*³⁵ suggesting *in vivo* biocompatibility of BC. Macroscopic inflammation signs such as exudate and edema were not observed around the grafted BC membrane, and foreign body and microscopic inflammation response induced by cellulose-based materials were negligible. The host tissue integrated suitably, and no chronic inflammatory reaction was found. In addition, during 4 weeks and 8 weeks of healing period, an amount of new bone formation in defect region loaded with BC membrane was similar to that of collagen membrane application. Moreover, a proper progression of new bone formation confirmed the efficacy of BC as a barrier membrane that secures and maintains space for bone regeneration.

Collagen membrane is widely used in clinics and noticed as a biodegradable membrane that exhibits great advantages such as excellent biocompatibility, feasible manageability, and especially no requirement for second surgery; therefore, a comparative study comparing BC membrane to collagen membrane was inevitable. BC membrane and collagen membrane used in the present study shared similar Scanning Electron Microscope images: the outer surface of both BC membrane and collagen membrane displayed an entangled porous structure made of nano-sized fibers, the cross-sectional surface showed a multilayered lamellar structure, and BCM exclusively presented an interconnected 3-dimensional structure of microfibrils between layers. This 3-D microfibril network is formed by holding cellulose chains of 20 - 50 nm nanofiber via hydrogen bond.³⁶ This particular holding allows outstanding extension strength, water retention capacity, and Young's modulus, and it accounts for a high degree of crystallinity, low solubility, and poor degradation of cellulose *in vivo*.^{35,36} Compared to collagen membrane, BCM showed significantly higher wet tensile stress, tensile strain, and Young's modulus. As Buser *et al.*⁹ reported mechanical strength of a barrier membrane as a key factor for successful GBR, the superior mechanical properties of BC membrane affect prominently on achieving stable bone tissue regeneration.

However, in spite of excellent mechanical properties,

water retention, and biodegradation of polymeric matrix, if the matrix doesn't exhibit bioactivity to support interaction with cells, it cannot be used as a barrier membrane for tissue engineering. Compared to synthetic polymers, biopolymers with naturally porous structure such as bacterial cellulose and collagen are renowned for their excellent biological function.³¹ Several factors should be considered thoroughly in order to achieve cell-occlusiveness and tissue integration as a barrier membrane: for instance, the porosity of a biopolymer has to block penetration of undesired tissues such as fibrous tissue and epithelial cells into bone defect while accepting and integrating essential tissues for angiogenesis and bone regeneration.⁹ Zellin and Linde³⁷ and Lundgren *et al.*³⁸ reported that compared to membranes with non-porous or reduced porosity, application of a membrane with porosity larger than 25 μm improved bone formation during initial healing period. Moreover, Zaborowska *et al.*³⁹ suggested that a barrier membrane with nanoporosity that is effective with cell attachment and osteoblastic differentiation and microporosity that enhances cell migration, transport of nutrients, cell cluster within the pores, and the formation of denser mineral deposits performs as an ideal scaffold for bone regeneration. In this experiment, 3-dimensional porous structure of BC membrane was observed to contain approximately 60% of porosity and the pore diameter of 26 μm , representing its highly porous structure compared to collagen membrane. However, after 7 days of cell culture *in vitro*, cell proliferation on the surface of BC membrane was measured to be lower than that on collagen membrane surface, and the attached cells on BC membrane were observed to exhibit polygonal morphology in contrast to cells on collagen membrane displaying noticeable f-actin stress fibers.

This morphological characteristic of cells was reported in the previous studies where BC was used.^{31,39-41} Mechanical and biologic properties of a commercial were enhanced via physical methods including gamma or ultraviolet radiation⁴² or chemical cross-linked methods including formaldehyde or glutaraldehyde.³¹ BC membrane also contains an outstanding 3-dimensional cross-linked structure formed by neutral porous nanofibrils. However, BC membrane drew weaker cell response than collagen membrane as observed in this experiment: the absence of charged groups in neutral polysaccharides of BC membrane enhances biocompatibility, but it poses negative influence on cell adhesion and proliferation efficacy due to lack of cell cognition.³⁹ Cell

adhesion can be accomplished when negative groups of cell surface get coupled with positive charges of membrane surface and the interaction between cell and membrane can be affected not only by charge density but also by crystallinity of membrane, arrangement of polymers, water absorption properties, surface morphology.³¹ In contrast to polymers used for other tissue engineering, a barrier membrane for GBR has to satisfy cell-occlusiveness and tissue integration. Thus, through observing more periodically over observation period, further studies on BC membrane should address inhibition of unwanted cell invasion, such as epithelial cells, and its excellent adhesion and proliferation of cells required for bone regeneration like osteoblasts.

Through *in vitro* experiment, BC membrane exhibited more decreased cell adhesion and differentiation than collagen membrane during the initial period; however, based on *in vivo* experiment analysis on bone regeneration at week 4 and 8 of delayed healing period, the degrees of bone regeneration in the both cases were comparable. As mentioned earlier, the studies by Zelline and Linde³⁷ and Lundgren *et al.*³⁸ reported that after 12 weeks of healing period, the total amounts of neogenetic bone of all types of membrane were similar. Based on the histological analysis of this experiment, mesenchymal cell, collagen fibrous connective tissue, osteoblast, osteoid, osteocyte in lacuna, bone matrix, and blood vessel were observed inside of the defect space separated by bacterial cellulose membrane. Transmembrane penetration of blood vessels which increases blood supply in GBR⁴³ was observed, and its pattern was different in the two membranes. While collagen membrane with multilayered lamellar structure showed a linear arrangement of blood vessels, BCM with cross-linked porous structure exhibited a packed and randomized arrangement of blood vessels. This blood vessel arrangement of BCM seems to encourage tissue regeneration.

The observation made at week 8 after applying BC membrane onto 8 mm calvarial defect area revealed the woven bone near the existing old bone at defect margin and a small amount of the lamellar bone. Inside the defect area, mesenchymal cells within a collagen fiber were scattered irregularly around bone graft materials, osteoblasts differentiated from mesenchymal cells created a lining, and the formation of osteoid around osteoblasts was observed. The healing process through intramembranous ossification was carried out comparably in both membranes. The grafted BC membrane did not induce inflammatory response; it integrated appropriately with the surrounding tissue, stabilized the defect area, and maintained adequate space for bone regeneration, satisfying the standards as a barrier membrane. However, observing twice at week 4 and 8 seems insufficient to evaluate inflammation during the initial stage of grafting, to predict the timing of complete biodegradation, and to assess new trabecular bone formation inside the defect. Thus, observations should be made more frequently and periodically, and an observation period should be long enough. Helenius³⁵ reported BC membrane not degraded after 12 weeks. Mårtson⁴⁴ who used rat model confirmed

softening and fragmentation of cellulose sponge after 16 weeks and designated the cellulose sponge not degraded completely after 60 weeks as “a slowly degradable implantation material.” Bacterial cellulose shows lower degradation due to its high crystallinity and the cellulose can be degraded naturally by fungal and microbial enzymes that execute hydrolase attack on β -(1,4) glycosidic bonds, but these cellulose enzymes do not exist in mammals.³¹ Along the availability of cellulose enzyme and crystallinity of cellulose, a rate of BC degradation depends on chemical components of a main chain and side groups, aggregation state and morphology of BC material, hydrophilic-hydrophobic balance, surface area, and other factors.³⁹ Therefore, further studies on regulating the rate of degradation are required.

Mandible and maxilla in which GBR method can be applied in clinical settings are flat bones; therefore, based on the experimental result from this study where rat calvarial flat bone defect was adopted, bone repair and remodeling through intramembranous ossification process can be predicted in these bones. However, in order to perform chairside application using BC as a barrier membrane, as Bottino *et al.*⁴⁵ mentioned, it is critical to design a defect model that replicates specific clinical conditions of alveolar bone in mandible and maxilla with larger animals and to assess true biomechanical integrity and biodegradation, healing, vascularization properties, and regeneration and remodeling.

CONCLUSION

In this study, application of bacterial cellulose membrane fabricated using biomimetic method on rat calvarial bone defect area was carried out comparably in collagen membranes. During healing period, a proper progression of new bone formation confirmed the efficacy of bacterial cellulose membrane as a barrier membrane.

ORCID

So-Hyun Lee <http://orcid.org/0000-0003-3094-6086>
 Chang-Mo Jeong <http://orcid.org/0000-0001-5009-9799>
 Jung-Bo Huh <http://orcid.org/0000-0001-7578-1989>

REFERENCES

1. Brånemark PI, Zarb GA, Albrektsson T. Tissue-integrated prostheses: Osseointegration in clinical dentistry. Chicago, Quintessence, 1985. p. 199-209.
2. Misch CM. Comparison of intraoral donor sites for onlay grafting prior to implant placement. *Int J Oral Maxillofac Implants* 1997;12:767-76.
3. Oda T, Sawaki Y, Ueda M. Experimental alveolar ridge augmentation by distraction osteogenesis using a simple device that permits secondary implant placement. *Int J Oral Maxillofac Implants* 2000;15:95-102.
4. Hämmerle CH, Karring T. Guided bone regeneration at oral implant sites. *Periodontol* 2000 1998;17:151-75.

5. Ashley FL, Stone RS, Alonsoartieda M, Syverud JM, Edwards JW, Sloan RF, Mooney SA. Experimental and clinical studies on the application of monomolecular cellulose filter tubes to create artificial tendon sheaths in digits. *Plast Reconstr Surg Transplant Bull* 1959;23:526-34.
6. Buser D, Halbritter S, Hart C, Bornstein MM, Grütter L, Chappuis V, Belser UC. Early implant placement with simultaneous guided bone regeneration following single-tooth extraction in the esthetic zone: 12-month results of a prospective study with 20 consecutive patients. *J Periodontol* 2009;80:152-62.
7. Schwarz F, Rothamel D, Herten M, Wüstefeld M, Sager M, Ferrari D, Becker J. Immunohistochemical characterization of guided bone regeneration at a dehiscence-type defect using different barrier membranes: an experimental study in dogs. *Clin Oral Implants Res* 2008;19:402-15.
8. Scantlebury TV. 1982-1992: a decade of technology development for guided tissue regeneration. *J Periodontol* 1993;64:1129-37.
9. Buser D, Dahlin C, Schenk RK. Guided bone regeneration in implant dentistry. Chicago, Quintessence, 1994. p. 32-4.
10. Sculean A, Nikolidakis D, Schwarz F. Regeneration of periodontal tissues: combinations of barrier membranes and grafting materials - biological foundation and preclinical evidence: a systematic review. *J Clin Periodontol* 2008;35:106-16.
11. Behring J, Junker R, Walboomers XF, Chessnut B, Jansen JA. Toward guided tissue and bone regeneration: morphology, attachment, proliferation, and migration of cells cultured on collagen barrier membranes. A systematic review. *Odontology* 2008;96:1-11.
12. Kasaj A, Reichert C, Götz H, Röhrig B, Smeets R, Willershausen B. In vitro evaluation of various bioabsorbable and nonresorbable barrier membranes for guided tissue regeneration. *Head Face Med* 2008;4:22.
13. Gentile P, Chiono V, Tonda-Turo C, Ferreira AM, Ciardelli G. Polymeric membranes for guided bone regeneration. *Biotechnol J* 2011;6:1187-97.
14. Polimeni G, Albandar JM, Wikesjö UM. Prognostic factors for alveolar regeneration: effect of space provision. *J Clin Periodontol* 2005;32:951-4.
15. Zhang J, Xu Q, Huang C, Mo A, Li J, Zuo Y. Biological properties of an anti-bacterial membrane for guided bone regeneration: an experimental study in rats. *Clin Oral Implants Res* 2010;21:321-7.
16. Jovanovic SA, Hunt DR, Bernard GW, Spiekermann H, Wozney JM, Wikesjö UM. Bone reconstruction following implantation of rhBMP-2 and guided bone regeneration in canine alveolar ridge defects. *Clin Oral Implants Res* 2007;18:224-30.
17. von Arx T, Buser D. Horizontal ridge augmentation using autogenous block grafts and the guided bone regeneration technique with collagen membranes: a clinical study with 42 patients. *Clin Oral Implants Res* 2006;17:359-66.
18. Fujihara K, Kotaki M, Ramakrishna S. Guided bone regeneration membrane made of polycaprolactone/calcium carbonate composite nano-fibers. *Biomaterials* 2005;26:4139-47.
19. Jung RE, Lecloux G, Rompen E, Ramel CF, Buser D, Hammerle CH. A feasibility study evaluating an in situ formed synthetic biodegradable membrane for guided bone regeneration in dogs. *Clin Oral Implants Res* 2009;20:151-61.
20. Schwarz F, Herten M, Ferrari D, Wieland M, Schmitz L, Engelhardt E, Becker J. Guided bone regeneration at dehiscence-type defects using biphasic hydroxyapatite + beta tricalcium phosphate (Bone Ceramic) or a collagen-coated natural bone mineral (BioOss Collagen): an immunohistochemical study in dogs. *Int J Oral Maxillofac Surg* 2007;36:1198-206.
21. Felipe ME, Andrade PF, Grisi MF, Souza SL, Taba M, Palioto DB, Novaes AB. Comparison of two surgical procedures for use of the acellular dermal matrix graft in the treatment of gingival recessions: a randomized controlled clinical study. *J Periodontol* 2007;78:1209-17.
22. Wang HL, MacNeil RL, Shieh AT, O'Neal R. Utilization of a resorbable collagen membrane in repairing gingival recession defects. *Pract Periodontics Aesthet Dent* 1996;8:441-8; quiz 450.
23. Dahlin C, Linde A, Gottlow J, Nyman S. Healing of bone defects by guided tissue regeneration. *Plast Reconstr Surg* 1988;81:672-6.
24. Shim JH, Huh JB, Park JY, Jeon YC, Kang SS, Kim JY, Rhie JW, Cho DW. Fabrication of blended polycaprolactone/poly(lactic-co-glycolic acid)/ β -tricalcium phosphate thin membrane using solid freeform fabrication technology for guided bone regeneration. *Tissue Eng Part A* 2013;19:317-28.
25. Kim SM, Lee JH, Jo JA, Lee SC, Lee SK. Development of a bioactive cellulose membrane from sea squirt skin for bone regeneration - a preliminary research. *J Korean Assoc Oral Maxillofac Surg* 2005;5:440-53.
26. Dugan JM, Gough JE, Eichhorn SJ. Bacterial cellulose scaffolds and cellulose nanowhiskers for tissue engineering. *Nanomedicine* 2013;8:287-98.
27. Embuscado ME, Marks JS, BeMiller JN. Bacterial cellulose. II. Optimization of cellulose production by *Acetobacter xylinum* through response surface methodology. *Food Hydrocoll* 1994;8:419-30.
28. Rainer J, Luiz FF. Production and application of microbial cellulose. *Polym Degrad Stab* 1998;59:101-6.
29. Busch O, Solheim E, Bang G, Tornes K. Guided tissue regeneration and local delivery of insulinlike growth factor I by bioerodible polyorthoester membranes in rat calvarial defects. *Int J Oral Maxillofac Implants* 1996;11:498-505.
30. Wan Y, Gao C, Han M, Liang H, Ren K, Wang Y, Luo H. Preparation and characterization of bacterial cellulose/heparin hybrid nanofiber for potential vascular tissue engineering scaffolds. *Polym Adv Technol* 2011;22:2643-8.
31. Nwe N, Furuike T, Tamura H. Selection of a biopolymer based on attachment, morphology and proliferation of fibroblast NIH/3T3 cells for the development of a biodegradable tissue regeneration template: Alginate, bacterial cellulose and gelatin. *Process Biochem* 2010;45:457-66.
32. Wan YZ, Huang Y, Yuan CD, Raman S, Zhu Y, Jiang HJ, He F, Gao C. Biomimetic synthesis of hydroxyapatite/bacterial cellulose nanocomposites for biomedical applications. *Mater*

Sci Eng C 2007;27:855-64.

33. Müller FA, Müller L, Hofmann I, Greil P, Wenzel MM, Staudenmaier R. Cellulose-based scaffold materials for cartilage tissue engineering. *Biomaterials* 2006;27:3955-63.
34. Tuzlakoglu K, Bolgen N, Salgado AJ, Gomes ME, Piskin E, Reis RL. Nano- and micro-fiber combined scaffolds: a new architecture for bone tissue engineering. *J Mater Sci Mater Med* 2005;16:1099-104.
35. Helenius G, Bäckdahl H, Bodin A, Nannmark U, Gatenholm P, Risberg B. In vivo biocompatibility of bacterial cellulose. *J Biomed Mater Res A* 2006;76:431-8.
36. Miyamoto T, Takahashi S, Ito H, Inagaki H, Noishiki Y. Tissue biocompatibility of cellulose and its derivatives. *J Biomed Mater Res* 1989;23:125-33.
37. Zellin G, Linde A. Effects of different osteopromotive membrane porosities on experimental bone neogenesis in rats. *Biomaterials* 1996;17:695-702.
38. Lundgren AK, Sennerby L, Lundgren D. Guided jaw-bone regeneration using an experimental rabbit model. *Int J Oral Maxillofac Surg* 1998;27:135-40.
39. Zaborowska M, Bodin A, Bäckdahl H, Popp J, Goldstein A, Gatenholm P. Microporous bacterial cellulose as a potential scaffold for bone regeneration. *Acta Biomater* 2010;6:2540-7.
40. Bäckdahl H, Helenius G, Bodin A, Nannmark U, Johansson BR, Risberg B, Gatenholm P. Mechanical properties of bacterial cellulose and interactions with smooth muscle cells. *Biomaterials* 2006;27:2141-9.
41. Fang B, Wan YZ, Tang TT, Gao C, Dai KR. Proliferation and osteoblastic differentiation of human bone marrow stromal cells on hydroxyapatite/bacterial cellulose nanocomposite scaffolds. *Tissue Eng Part A* 2009;15:1091-8.
42. Fujimori E. Ultraviolet light-induced change in collagen macromolecule. *Biopolym* 2004;3:115-9.
43. Rothamel D, Schwarz F, Fienitz T, Smeets R, Dreiseidler T, Ritter L, Happe A, Zöller J. Biocompatibility and biodegradation of a native porcine pericardium membrane: results of in vitro and in vivo examinations. *Int J Oral Maxillofac Implants* 2012;27:146-54.
44. Märtson M, Viljanto J, Hurme T, Laippala P, Saukko P. Is cellulose sponge degradable or stable as implantation material? An in vivo subcutaneous study in the rat. *Biomaterials* 1999;20:1989-95.
45. Bottino MC, Thomas V, Schmidt G, Vohra YK, Chu TM, Kowolik MJ, Janowski GM. Recent advances in the development of GTR/GBR membranes for periodontal regeneration-a materials perspective. *Dent Mater* 2012;28:703-21.